BioOne COMPLETE

Elemental Distribution in Reproductive and Neural Organs of the Epilachna nylanderi (Coleoptera: Coccinellidae), a Phytophage of Nickel Hyperaccumulator Berkheya coddii (Asterales: Asteraceae) by micro-PIXE

Authors: Mesjasz-Przybyłowicz, Jolanta, Orłowska, Elżbieta, Augustyniak, Maria, Nakonieczny, Mirosław, Tarnawska, Monika, et al.

RESEARCH

Elemental Distribution in Reproductive and Neural Organs of the *Epilachna nylanderi* (Coleoptera: Coccinellidae), a Phytophage of Nickel Hyperaccumulator *Berkheya coddii* (Asterales: Asteraceae) by micro-PIXE

Jolanta Mesjasz-Przybyłowicz,[1] Elżbieta Orłowska,[1,2] Maria Augustyniak,[3] Mirosław Nakonieczny,[3] Monika Tarnawska,[3] Wojciech Przybyłowicz,[1,4] and Paweł Migula[3,5]

[1]Materials Research Department, iThemba LABS, National Research Foundation, P.O. Box 722, Somerset West 7129, South Africa
[2]Department of Molecular Biology and Genetics, University of Aarhus, Gustav Wieds Vej 10 C, Aarhus C 8000, Denmark
[3]Department of Animal Physiology and Ecotoxicology, University of Silesia, Bankowa 9, Katowice 40-007, Poland
[4]AGH University of Science and Technology, Faculty of Physics & Applied Computer Science, al. A. Mickiewicza 30, Kraków 30-059, Poland
[5]Corresponding author, e-mail: pawel.migula@us.edu.pl

ABSTRACT. The phenomenon of metal hyperaccumulation by plants is often explained by a pathogen or herbivore defense hypothesis. However, some insects feeding on metal hyperaccumulating plants are adapted to the high level of metals in plant tissues. Former studies on species that feed on the leaves of *Berkheya coddii* Roessler 1958 (Asteraceae), a nickel-hyperaccumulating plant, demonstrated several protective mechanisms involved in internal distribution, immobilization, and elimination of Ni from the midgut and Malpighian tubules. These species are mainly coleopterans, including the lady beetle, *Epilachna nylanderi* (Mulsant 1850) (Coleoptera: Coccinellidae), collected from the ultramafic ecosystem near Barberton in South Africa. By performing particle-induced X-ray emission microanalysis elemental microanalysis (PIXE), this study examined whether Ni may be harmful to internal body systems that decide on insect reactivity (central nervous system [CNS]), their reproduction, and the relationships between Ni and other micronutrients. Data on elemental distribution of nine selected elements in target organs of *E. nylanderi* were compared with the existing data for other insect species adapted to the excess of metals. Micro-PIXE maps of seven regions of the CNS showed Ni mainly in the neural connectives, while cerebral ganglia were better protected. Concentrations of other bivalent metals were lower than those of Ni. Testis, compared with other reproductive organs, showed low amounts of Ni. Zn was effectively regulated at physiological dietary levels. In insects exposed to excess dietary Zn, it was also accumulated in the reproductive organs. Comparison of *E. nylanderii* with other insects that ingest hyperaccumulating plants, especially chrysomelid *Chrysolina clathrata* (Clark) (Coleoptera: Chrysomelidae), showed lower protection of the CNS and reproductive organs.

Key Words: Ni-hyperaccumulating plant, elemental distribution, X-ray microanalysis, nuclear microprobe, plant-insect interaction

The phenomenon of metal hyperaccumulation by plants is often explained by the elemental defense hypothesis (Boyd 2004, 2007; Boyd and Martens 1998). This hypothesis suggests that maintaining high levels of heavy metal in aboveground organs of the plant may have evolved to defend hyperaccumulating plants against some natural enemies, such as herbivores and pathogens. To counteract this plant defense, some herb-grazing insects have evolved various physiological, ecological, and behavioral strategies to minimize toxic effects of metals in their diet (Vijver et al. 2004). Because of these adaptations, some herbivorous insects can use hyperaccumulating plants as the major part of their diet (Mesjasz-Przybyłowicz and Przybyłowicz 2001, Peterson et al. 2003, Boyd 2004, Jhee et al. 2006, Migula et al. 2007, Boyd 2009). Knowledge of the physiological mechanisms driving metal tolerance in insects is still limited. Studying specific mechanisms of metal tolerance will broaden understanding of coevolution between hyperaccumulating plants and their grazers in ultramafic ecosystems, and ecosystems contaminated with metals. An excess of consumed metals might become toxic, and these insects must prevent, decrease, or repair the effects of metals that have entered their bodies.

Berkheya coddii Roessler 1958 (Asterales: Asteraceae), an endemic plant species from ultramafic ecosystems, is one of five Ni hyperaccumulators from South Africa, for which several associated herbivorous insect species able to utilize metalliferous plant material without any significant effects on their population dynamics have been reported (Morrey et al. 1989, Mesjasz-Przybyłowicz and Przybyłowicz

2001, Migula et al. 2007, Boyd 2009). Among them, two coleopteran species—the chrysomelid leaf beetle (*Chrysolina clathrata* (Clark), (Coleoptera: Chrysomelidae), formerly *Chrysolina pardalina* Fabricius, 1781) and the lady beetle (*Epilachna nylanderi*) (Mulsant 1850) (Coleoptera: Coccinellidae)—and the grasshopper (*Stenoscepa* sp.) have been the subjects and the objects of intensive structural, physiological, and ecological studies, including elemental microanalysis using the particle-induced X-ray emission microanalysis (PIXE) (Mesjasz-Przybyłowicz et al. 2002; Przybyłowicz et al. 2003, 2004, 2005; Augustyniak et al. 2002, 2006, 2008; Nakonieczny 2007; Migula et al. 2011). Elemental distributions in the whole body and in the isolated body organs were obtained (Przybyłowicz et al. 2004). In previous studies, the importance of the target organs as the first line of defense against excessive amounts of metals has been demonstrated. Several structural and morphological adaptations to utilize the Ni-rich leaves of *B. coddii* were found in *C. clathrata* and *Stenoscepa* sp. The most important structural and functional adaptations took place in the midgut and Malpighian tubules. Most of the consumed nickel is directly rejected from the gut. Ni accumulated in granular concretions of the epithelial midgut cells is eliminated during apoptosis of these cells (Klag et al. 2002; Przybyłowicz et al. 2004, 2005; Augustyniak et al. 2006, 2008; Nakonieczny 2007). *E. nylanderi* belongs to the group that easily modifies their food preferences (Giorgi et al. 2009). Former studies on this species searched for mechanisms involved in distribution, immobilization, and decontamination of nickel from the midgut and Malpighian tubules and other forms of Ni elimination (Przybyłowicz

et al. 2005, Nakonieczny 2007; Makgale 2008; Rost-Roszkowska et al. 2008, 2010; Migula et al. 2011).

Toxicokinetic processes help to determine how much of a toxic substance reaches insect target organs, where the substances entered the organism, and the internal distribution and metabolism of these substances (Migula 1996, Przybyłowicz et al. 2004, Vijver et al. 2004, Mesjasz-Przybyłowicz and Przybyłowicz 2011). Excess of Ni may change the balance between microelements in the internal organs of insects (Mesjasz-Przybyłowicz et al. 2002, Migula et al. 2004, Augustyniak et al. 2008). Both species of beetles mentioned above can maintain Ni body levels that are toxic to related species that feed on nonaccumulating Ni plant species (Nakonieczny 2007). Detailed analysis using the micro-PIXE method indicated an uneven distribution of metals in *C. clathrata*, from $0.8\,\mu g\,g^{-1}$ of Ni in the fat body to $3,000\,\mu g\,g^{-1}$ in the Malpighian tubules (Przybyłowicz et al. 2003, 2005; Nakonieczny 2007). Analysis of Ni concentration and distribution in the reproductive organs and brain ganglia of this species indicated that these organs were sufficiently protected against Ni toxicity (Przybyłowicz et al. 2003). It is not known whether the distribution of trace elements in the open circulatory system of *E. nylanderi* may be harmful to other body organs responsible for life history traits and reproductive potential.

The aim of this study is to examine whether both the internal organs that control fast functional responses (central nervous system [CNS]) and the reproduction of insects are effectively protected against excess dietary nickel, and to determine the relationships between Ni and other micronutrients. Quantitative and qualitative data on elemental distribution in these target organs of *E. nylanderi* were compared with the existing data obtained for other insect species associated with Ni-hyperaccumulating plant species.

Materials and Methods

Adult beetles of *E. nylanderi* were collected from the ultramafic outcrops near Barberton (Mpumalanga Province, South Africa) as described elsewhere (Augustyniak et al. 2002, Migula et al. 2011). *E. nylanderii* underwent four instars and complete development within 17–31 d. Adults emerge after 3 wk of pupation and continue feeding on *B. coddii* leaves, consuming only their soft epidermal and parenchymal parts (Migula et al. 2011).

Sample Preparation for Elemental Microanalysis. Material was sectioned from insects starved for 24 h to empty their guts of the remains of ingested food. Similar to former studies describing elemental distribution in the gut and Malpighian tubules, the CNS and the male internal reproductive organs were isolated from the same group of beetles for further analysis (Przybyłowicz et al. 2005, Nakonieczny 2007, Migula et al. 2011).

Zn and Ni, according to the biological classification of Nieboer and Richardson (1980), belong to the border class of metals that have no binding preference and form ligands with many functional groups (sulfur containing or oxygen containing). Ni interacts with Zn, which in high concentrations is also toxic. Replacement of Zn by Ni may lead to enhanced toxicity. On the other hand, Zn in excess may exert a protective role against the stimulatory role of Ni in production of hydroxyl radicals (Nakonieczny 2007). This was the reason why a group of insects was also kept in the laboratory on *B. coddii* leaves presoaked in tap water containing 0.1 mM Zn for 1 wk, to study how an additional stressor might affect the redistribution of elements in the analyzed samples.

Isolated internal organs were immediately preserved by cryofixation against a cold metal block and freeze-dried. Lyophilized samples were mounted between the two formvar film layers (Przybyłowicz et al. 2005).

Elemental Microanalysis. Microanalyses were carried out using the nuclear microprobe at the Materials Research Department, iThemba LABS, South Africa, as described previously (Prozesky et al. 1995; Przybyłowicz et al. 1999, 2005). A proton beam of 3-MeV energy, generated by the 6-MV single-ended Van de Graaff accelerator, was focused to a 3 by 3 μm^2 spot and raster scanned over selected areas of analyzed samples, using square or rectangular scan patterns with a variable number of pixels (up to 128 by 128). Proton current was restricted to 200–300 pA to minimize specimen beam damage. Particle-induced X-ray emission (PIXE) and proton backscattering spectrometry (BS) were used simultaneously. PIXE spectra were registered with an Si(Li) Link Pentafet detector (80-mm^2 active area and 8-μm Be window) with an additional 190-μm Kapton layer as an external absorber. The effective energy resolution of the PIXE system (for the Mn Kα line) was 165–170 eV, measured for individual spectra. The detector was positioned at a take-off angle of 135° and a working distance of 25 mm. The X-ray energy range was set between 1 and 36 keV. BS spectra were recorded with an annular Si surface barrier detector (100 μm thick) positioned at an average angle of 176°. Data were acquired in the event-by-event mode. The normalization of results was done using the integrated beam charge and collected simultaneously from a Faraday cup located behind the specimen and from the insulated specimen holder. The total accumulated charge per scan varied from 1 to 5 μC. Overall, 53 scans were performed.

Quantitative results were obtained by a standardless method using GeoPIXE II software package (Ryan et al. 1990, Ryan 2000). The error estimates are extracted from the error matrix generated in the fit, and the minimum detection limits are calculated using the Currie equation (Currie 1968). The detailed calibration of detector efficiency, the thicknesses of selectable X-ray attenuating filters, and studies on the accuracy and precision have been reported elsewhere (Van Achterbergh et al. 1995). The procedure reported there was used for the Link Si(Li) detector used in this study. The calibration of the analytical system was tested by measurements of standards—pure elements and synthetic glasses with known quantities of selected minor elements (internal standards), the X-ray peaks of which cover practically the whole measurable energy range. Quantitative elemental mapping was performed using a dynamic analysis method (Ryan and Jamieson 1993, Ryan et al. 1995, Ryan 2000). This method generates elemental images that are 1) overlap resolved; 2) with subtracted background; and 3) quantitative, i.e., accumulated in mg kg^{-1} dry weight units. Maps were constructed using matrix composition and areal density representative of the scanned area.

In addition, average elemental concentrations from specific selected regions drawn over the main structures of dissected body parts of adult *E. nylanderi* were obtained. These concentrations were obtained using a full nonlinear deconvolution procedure to fit PIXE spectra (Ryan et al. 1990), with matrix corrections based on areal density and matrix composition obtained from the corresponding BS spectra, fitted with a RUMP simulation package (Doolittle 1986) with non-Rutherford cross-sections for C, O, and N. Matrix corrections done on the basis of BS results were essential due to the variable thickness of analyzed specimens. Elemental concentrations from these areas are also reported in mg kg^{-1} dry weight.

Of 16 measured elements, the data for 9 elements (S, Cl, K, Ca, Fe, Ni, Mn, Cu, and Zn), for which all levels were above the accepted 99% detection limits, were presented in maps and appropriate tables, and interpreted.

Statistical procedures were performed using the Statistica v.10 software package for personal computer. The means and SD were calculated from multiple scans across the 3 by 3 grid. Significance of means within the same element and between the species was analyzed using one-way analysis of variance and least significant difference tests, at $P < 0.05$.

Results

The Central Nervous System. The CNS of *E. nylanderi* is similar to other beetle species and consists of the brain with three fused ganglionic masses (proto-, deuto-, and tritocerebrum), three ventral ganglia (pro-, meso-, and metathoracic), abdominal ganglia, and the ventral
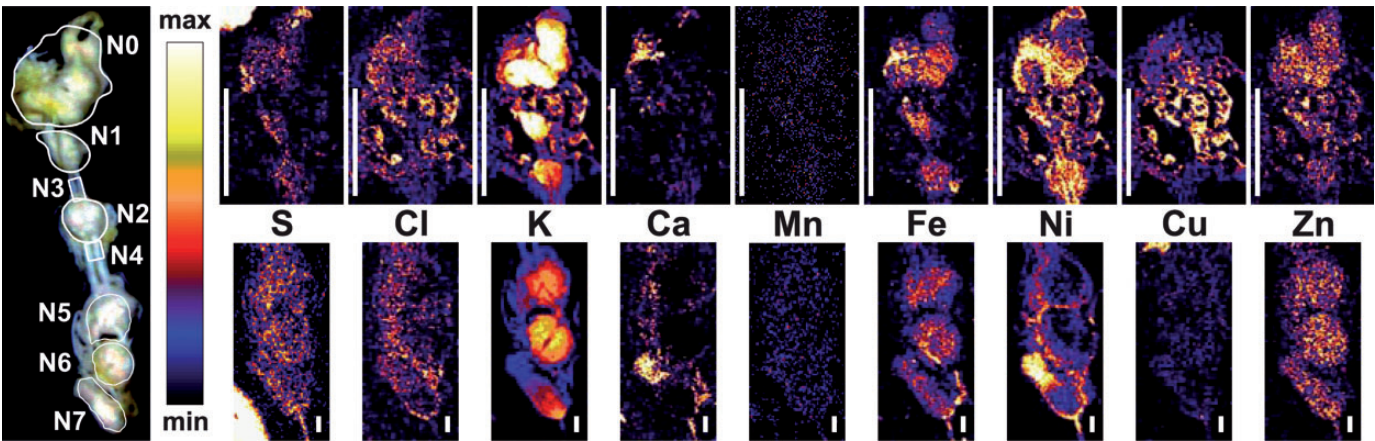
Fig. 1. Elemental distribution in the central nervous system (CNS) of *Epilachna nylanderi*. The first image on the left: light micrograph of lyophilized sample with selected regions: N0, left optic lobes and protocerebrum; N1, deuto- and tritocerebrum; N2, first thoracic gland; N3, paired giant connectives; N4, paired giant connectives; N5, second thoracic gland; N6, third thoracic gland; N7, part of the hindgut. Micro-PIXE visualization of the distribution of nine elements in selected regions of the CNS is shown in two rows. Scale = 1 mm (white bars on the left side in the images of the upper row) and 0.1 mm (white bars on the right side of the images in the bottom row).

Table 1. Concentration of selected elements (mean ± SD in mg kg⁻¹) in various parts of the central nervous system of the adult *Epilachna nylanderi*

Region	S	Cl	K	Ca	Mn	Fe	Ni	Cu	Zn
N0	4,620 ± 830a (273)	1,550 ± 14a (48)	11,080 ± 92a (7.5)	292 ± 21a (4.9)	1.3 ± 0.8a (1.3)	96 ± 2a (1)	144 ± 3a (1.5)	247 ± 3a (1.5)	57 ± 1a (1.4)
N1	4,720 ± 840a (675)	2,050 ± 140b (119)	13,970 ± 120c (19)	251 ± 18a (13)	4 ± 2a (3.5)	114 ± 4a (2.9)	161 ± 6a (4.6)	506 ± 12b (4.6)	59 ± 4a (3.7)
N2	3,990 ± 810a (636)	1,270 ± 116a (2)	9,320 ± 100b (4.1)	316 ± 28a (2.7)	10 ± 2b (0.7)	110 ± 3a (0.6)	248 ± 8b (6)	211 ± 6a (6)	60 ± 6a (0.6)
N3	8,700 ± 1,400a (848)	2,150 ± 270b (422)	10,300 ± 220a (72)	340 ± 56a (47)	12 ± 5b (8.6)	114 ± 12a (9.5)	420 ± 38c (19)	255 ± 35a (25)	48 ± 16 (30)
N4	11,200 ± 1,700b (607)	2,080 ± 350b (279)	9,010 ± 140b (65)	488 ± 73b (4)	14 ± 7b (12)	84 ± 10a (9.8)	518 ± 27c (16)	156 ± 18a (21)	40 ± 14a (25)
N5	4,510 ± 790a (319)	795 ± 99c (55)	12,840 ± 63c (9.4)	162 ± 22c (6.6)	3.6 ± 0.8a (1.7)	87 ± 2a (1.4)	147 ± 2a (1.7)	17 ± 1c (1.6)	49 ± 2a (1.6)
N6	5,030 ± 930a (351)	840 ± 110c (59)	14,910 ± 97c (10)	129 ± 24c (7)	2 ± 1a (1.8)	91 ± 2a (1.4)	122 ± 3a (1.7)	11.6 ± 1c (1.7)	53 ± 2a (1.5)
N7	4,440 ± 1,070a (365)	930 ± 160c (63)	10,300 ± 110a (12)	287 ± 21a (7.9)	4 ± 1a (2.2)	101 ± 2a (1.8)	395 ± 6c (2.2)	12 ± 1c (2.2)	53 ± 2a (1.9)

Data are obtained from PIXE spectra from these regions using a full nonlinear deconvolution procedure. Detection limits (99%) are given in parentheses. Selected regions are as shown in Figure 1: N0, left optic lobes and protocerebrum; N1, deuto- and tritocerebrum; N2, first thoracic gland; N3, paired giant connectives; N4, paired giant connectives; N5, second thoracic gland; N6, third thoracic gland; N7, part of the hindgut. Different letters denote significant differences between selected regions at $P < 0.05$.

nerve cord. The protocerebrum is the main integrative center and controls insect vision. The deutocerebrum receives information from sensory receptors in antennae and controls motoric activity of these organs. The tritocerebrum is the main autonomous center of the brain that closely cooperates with the subesophageal ganglion. Thoracic ganglia receive sensory receptors from appropriate pairs of legs and send motor axons to the leg muscles. Moreover, the second and third thoracic ganglia send their axons to the wing muscles (Nation 2001).

Elemental distribution was examined in seven regions of the CNS (Fig. 1; Table 1). Only the subesophageal parts in the head and the ventral abdominal ganglia were not analyzed separately.

Sulfur had a similar quantitative distribution in all analyzed neural ganglia (N0, N1, N2, N5, and N6), but its concentration was much higher in the areas of interganglionic neural connectives (N3 and N4). The distribution pattern of Cl was similar to that of S. Concentration of K in the selected neural structures was the highest within the analyzed elements. The mean value of K varied between 9,010 and 14,910 mg kg⁻¹ in neural connectives and the third thoracic gland. The mean coefficient of variation was low (0.07). The highest concentration

of K was maintained in the main brain ganglia and in the thoracic ganglia (Table 1). The lowest values were found in the areas of interganglionic connectives (N3, N4) and the first thoracic gland (N2). These structures were characterized by the highest Ca levels. Mn concentrations were the lowest of all examined elements. The coefficient of variation for Mn (0.34) was three times higher than for Ca (0.11). The concentration of Fe in the examined neural structures was kept at similar, insignificant levels. The average concentration of Ni in the CNS was 251.2 ± 8.2 mg kg⁻¹, and the highest levels were in the neural connectives (N4 and N3), as was the case for Ca. In these structures, Ni concentration was about three times higher than in the protocerebrum (N0). Cu was unevenly distributed, with low coefficients of variation, between 0.012 and 0.09. The maximal Cu concentration was 40 times higher than the minimal value. The distribution of Zn was more homogenous, and the difference between the minimal and maximal concentrations in a given area was not higher than 50%. Concentrations reached by the bivalent metals in comparison to Ni (= 1.0) could be placed in the following decreasing order: Ca (1.1), Cu (0.8), Fe (0.39), Zn (0.21), and Mn (0.027).
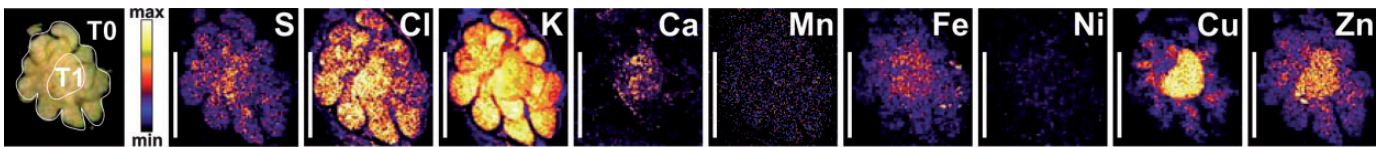
Fig. 2. Light micrograph with selected distal (T0) and basal (T1) regions and the distribution of elements in testicular follicles of *Epilachna nylanderi* (the first left image) are shown. Micro-PIXE visualization of the distribution of nine elements in selected regions of the testicular follicles. Scale (white bars on the left side of the images) = 1 mm.

Table 2. Concentration of selected elements (mean ± SD in mg kg^{-1}) in testes of the adult *Epilachna nylanderi*

Region	S	Cl	K	Ca	Mn	Fe	Ni	Cu	Zn
T0	10,400 ± 630a (130)	5,060 ± 180 (21)	15,000 ± 480a (4.6)	237 ± 49a (3.1)	3.4 ± 0.4a (0.8)	46 ± 1 (0.6)	3.3 ± 0.5 (0.8)	143 ± 2a (0.8)	85 ± 3a (0.8)
T1	16,500 ± 1,000b (310)	5,810 ± 220 (46)	11,800 ± 410b (8.6)	440 ± 46b (5.9)	1.2b (1.2)	57 ± 2 (1)	3.2 ± 0.7 (1.3)	360 ± 3b (1.4)	131 ± 3b (1.5)

Selected regions cover distal (T0) and basal (T1) regions of follicles. Data are obtained from PIXE spectra from these regions (shown in Fig. 2) using a full nonlinear deconvolution procedure. Detection limits (99%) are given in parentheses. Different letters denote significant differences between selected regions at $P < 0.05$.

Internal Reproductive Organs. The male internal reproductive system of the genus *Epilachna* is composed of a pair of testes, the vas deferens, the seminal vesicles ejaculatory duct, and four accessory glands (Davey 1985). The testes, as in many coleopteran species, are tuft shaped and built of many thick testicular follicles. Spermatogonia are located in a distal part of each follicle and after mitotic divisions form spermatocytes, grow, and pass toward the basal part of the follicle. In this region, cells undergo meiosis and mature spermatozoids are formed. Sperm produced in testicular follicles is stored in oval seminal vesicles, which in the case of *Epilachna* form separate structures. In the sampled material, two main areas were selected and were indicated as the basal T1 and distal T0 regions (Fig. 2; Table 2). A short vas eferens connects each testicular follicle with the vas deferens. This part of the testis covers the T1 area. Significant differences between regions were found for S, K, Ca, Mn, Cu, and Zn. The basal part of the testis was richer in S, Ca, Cu, and Zn in comparison with the distal part. The concentrations of Ca and Cu in the basal area were nearly twice as high. The distribution of the remaining elements (Cl, Fe, and Ni) was similar in both regions. It is worth to mentioning that in comparison with other reproductive organs, Ni in the testis was present in extremely low amounts.

Other parts of the reproductive tract—the tube-shaped vasa deferentia—are thick, built of external epithelium laid on basal lamina, and covered inside with circular muscles. They are long and create loops in the body cavity, ending in a single ejaculatory duct. The accessory glands make a junction with vasa deferentia. They produce and release various protein compounds involved in production of spermatophore and specific pheromones. Maps of elemental for these parts of the internal male reproductive system were complemented by average concentrations in the specific regions (Fig. 3; Table 3). For better visualization of joint Ni and Zn effects, the sample was taken from the group of insects kept on *B. coddii* leaves contaminated with Zn in the laboratory experiment. Concentrations of elements in the reproductive organs of *E. nylanderi* fed on control leaves uncontaminated with Zn are given in Table 4. Apart from S and Cl in seminal vesicles (R2), levels of other elements were lower than in the transporting tubes (R1) or in the accessory glands (R3; Table 3). The high Zn concentration reflected its high bioaccumulation rates from ingested food. Bioaccumulation factor is defined as the ratio of concentration of a chemical in an animal and concentration of the same chemical in its food. The rate was measured in a series of insect species associated with *B. coddii* (Migula et al. 2007). Our measurements indicated that bioaccumulation factor for Ni in these species was below 0.05 but much higher for other metals, including Zn (Zn > 2; Fe > 5). The average Zn concentration in insects not treated with excess of Zn was more than 70 times lower than that of Zn-treated insects (Table 4).

The bioconcentration factor of Ni in all the analyzed organs was low. The ratios of Ni concentrations in the examined organs for the non-Zn-treated to the Zn-treated insects (mesophyll of *B. coddii* leaves) were as follows: midgut, 0.02; Malpighian tubules, 0.007; CNS, 0.014; testis, 0.0002; and internal reproductive organs, 0.004.

Discussion

Effects of dietary Ni in insects associated with Ni-hyperaccumulating plants are difficult to compare with those in Ni-sensitive insects. Tests of choice showed that such plant material is unpalatable to most species. Their starvation induces degeneration processes; body weight is lost and it leads to insect death. Nakonieczny (2007) compared structural and functional adaptations of *C. clathrata* to an Ni-rich diet (leaves of *B. coddii*) with *Chrysolina herbacea* kept on Ni-enriched leaves of *Mentha* species. *C. herbacea* restricted feeding at 1,000 times lower concentration of Ni in the diet than *C. clathrata* and was not able to eliminate excessive Ni from the body. Its detoxifying system was also less effective than that of *C. clathrata*. Zawisza-Raszka and Doleżych (2008) showed that fewer than 50% of the *Spodoptera exigua* larvae fed Ni-contaminated leaves (900 mg kg^{-1}) reached the pupal stage. Similar Ni effects were observed in the leaf-mining larvae, *Eriocrania semipurpurella* (Kozlov et al. 2000). The low rate of Ni bioaccumulation of this species was concomitant with increased concentrations of the metal, decreased efficiency of feeding, and reduction of the body weight.

Nickel and Essential Micronutrients in *E. nylanderi*. The trace elements' feeding requirements are known only for a few insect species (Nation 2001). Insects have evolved various physiological mechanisms that regulate levels of essential ions such as K, Ca, Mn, Zn, Fe, or Cu (Bagatto and Shorthouse 1996). All elements (except Ni) analyzed in *E. nylanderi* were essential micronutrients. Body levels of these metals did not deviate much from those of other insects (Mattson and Scriber 1986).

Organisms must maintain adequate supplies of Fe to meet nutritional requirements while controlling their potential toxic property. Iron is transported to hemolymph by the transferrin and stored in the nontoxic ferritin. This complex is distributed further to various compartments of an insect cell (Nichol et al. 2002). When in excess, iron produces reactive oxygen species that may damage cellular membrane components or nucleic acids (Nichol et al. 2002, Green et al. 2010). In various coleopteran species, the Fe level oscillated around 100 mg kg^{-1} dry mass (Levy and Cromroy 1973, Mattson and Scriber 1986,
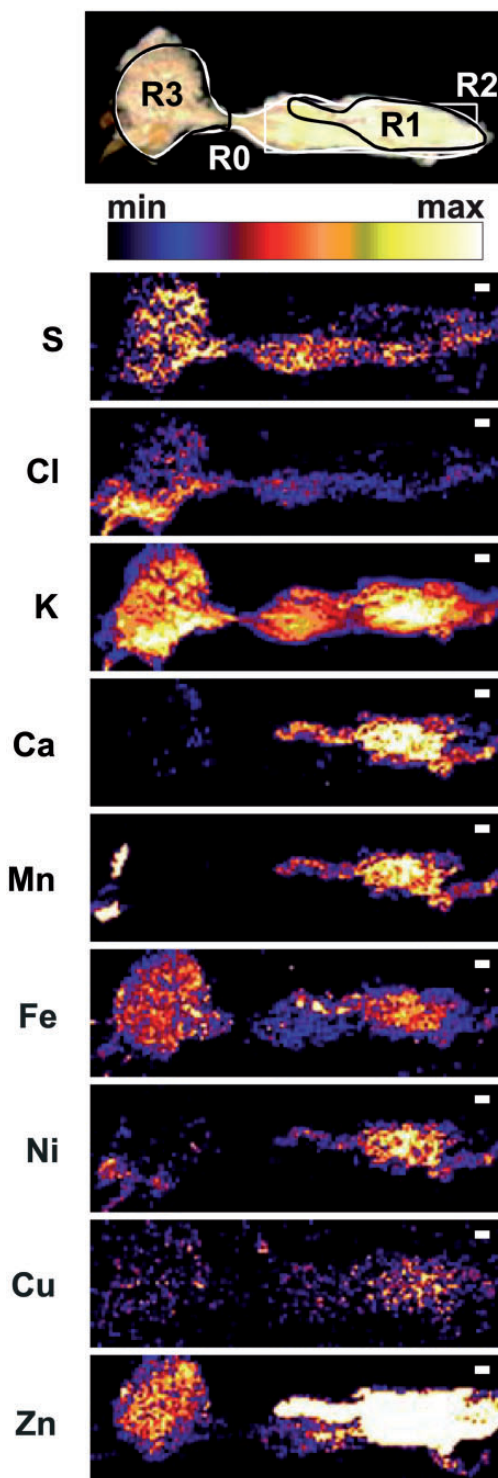
Fig. 3. The first image on the top: light micrograph image of the reproductive system of the adult *Epilachna nylanderi* male with selected regions: R0, a whole region covering male reproductive organs (without testes)—accessory gland with vas deferens, seminal vesicles, vas efferens, and ejaculatory duct; R1, vas deferens, vas efferens, and ejaculatory duct; R2, seminal vesicles; R3, accessory gland. The images below: Micro-PIXE visualization of the distribution of nine elements in selected regions of the male reproductive system. Scale (white bar on the top right side of each image) = 0.1 mm.

Tabashnik and Slansky 1986). Concentrations of Fe in organs of *E. nylanderi* do not differ from those in another coleopteran species—*C. clathrata* (Table 4). Beanland et al. (2003) found that another ladybird species, *Epilachna varivestis*, gained weight proportionally to the presence of Fe and Zn. Fe concentrations in other groups of Ni-adapted insects were organ dependent. In the brain of grasshoppers, *Stenoscepa* sp., it was only 64.8 ± 0.3 mg kg^{-1} (Augustyniak et al. 2008). Nearly the same Fe concentrations were found in the brain of *Chorthippus brunneus* (Orthoptera) inhabiting uncontaminated grassland (Augustyniak et al. 2006). Similar Fe concentrations were found in the head sap feeders of *B. coddii*: an aphid, *Protaphis pseudocardui* (62 ± 0.2 mg kg^{-1}), and a leafhopper, *Norialsus berkheyae* (43 ± 2 mg kg^{-1}) (Migula et al. 2007). The observations imply that regulatory mechanisms of Fe in Ni-adapted insects are not species specific.

Green et al. (2010) stated that if dietary Zn is given in excess to lady beetles, metal concentrations remain in the body at rather constant levels, whereas Ni and Cu are quickly rejected. This finding was not confirmed in the case of *E. nylanderi* exposed to high Zn dietary levels, for which excess of this metal was an additional stressor accumulating at high levels in the target organs (Table 4). The elimination rate of zinc from the insect body is high (Kramarz 1999). In case of *E. nylanderi*, the time left for depuration of the gut (24 h) was too short for the effective bioelimination of the metal.

Copper was present at levels high enough for the proper functioning of the reproductive organs and the CNS. These concentrations were much higher than reported in other coleopteran species inhabiting metal-contaminated areas (Migula et al. 2004). Comparisons with *C. clathrata* demonstrated similarities of the Cu burden in the reproductive organs and in the brain ganglia but differences in Malpighian tubules, confirming regulatory importance of this organ in maintaining proper levels of the metal (Table 4). It is worth mentioning that at high concentrations, copper can also participate in the production of free radicals (Valko et al. 2005, Das et al. 2008).

Nickel in Target Organs of *E. nylanderi*—A Comparison With Other Insect Species. Ni is generally a nonessential element in insect physiology. In insect species living in Ni-uncontaminated areas, it is weakly regulated. This metal could reach cells as a cotransporter in calcium channels. Accumulation of Ni depends on the genes responsible for specific metal transporter protein 1 synthesis (Nunez et al. 2010). Low Fe or Cu levels upregulate expression of this gene (Chung et al. 2004, Troadec et al. 2010).

Insect species living on ultramafic sites have had enough time to cope with an excess of Ni and evolve various physiological, morphological, and behavioral adaptations allowing control of Ni levels. The main strategy used by *E. nylanderi* against excess dietary Ni is its effective direct elimination from the gut. Ni is inactivated in granular concretions present in the midgut epithelial cells. These short-lived cells could easily move through apoptotic or necrotic pathways and are eventually eliminated with feces. Lost cells are quickly replaced by the new ones developed from regenerative cells, rich in number, in the midgut epithelium (Rost-Roszkowska et al. 2008, 2010; Migula et al. 2011). They could also use a similar mechanism, as described in *C. clathrata*, which effectively eliminates Ni through transmembrane transport: from the anterior part of midgut into the hindgut with the help of the Malpighian tubules (Przybyłowicz et al. 2005, Nakonieczny 2007).

Elemental maps of *E. nylanderi* testis (Fig. 2) indicated that this organ is well protected against excess Ni and at the same time maintains concentrations of other elements allowing homeostasis, necessary either of the part of intensive division of the germ cells (T0) or in the areas of their differentiation and transportation to seminal vesicles (T1). Despite this, quantitative relations between Ni and other determined metals differ between analyzed organs. Compared with testis (Fig. 4; Table 2), the mean concentrations of Ni in other selected reproductive organs were more than 11 and 17 times higher in insects kept on a diet without and with an excess of Zn, respectively (Table 4). Worth mentioning is that successful protection of generative organs against excess of dietary Ni in

Table 3. Concentration of selected elements (mean $\pm$ SD in mg kg^{-1}) in various parts of reproductive system of the adult male of *Epilachna nylanderi*

Region	S	Cl	K	Ca	Mn	Fe	Ni	Cu	Zn
R0	3,890 $\pm$ 510 (118)	926 $\pm$ 44 (21)	4,310 $\pm$ 26b (4.5)	2,610 $\pm$ 9c (3.3)	157 $\pm$ 2c (0.9)	135 $\pm$ 1a (0.7)	39 $\pm$ 1c (0.9)	13.6 $\pm$ 0.7b (1.2)	2,760 $\pm$ 29c (1.3)
R1	3,260 $\pm$ 600 (268)	861 $\pm$ 50 (44)	5,840 $\pm$ 53a (12)	8,400 $\pm$ 57a (7.6)	520 $\pm$ 5a (2.3)	179 $\pm$ 4b (2)	111 $\pm$ 4a (3)	23 $\pm$ 2a (4.5)	10,940 $\pm$ 120a (5.0)
R2	3,660 $\pm$ 390 (127)	850 $\pm$ 300 (2)	2,700 $\pm$ 17c (4.1)	414 $\pm$ 9d (2.7)	49 $\pm$ 0.6d (0.7)	90 $\pm$ 0.8c (0.6)	12 $\pm$ 0.4d (6)	7.5 $\pm$ 0.4c (6)	75 $\pm$ 0.9d (0.6)
R3	3,350 $\pm$ 560 (191)	821 $\pm$ 55 (33)	5,050 $\pm$ 33a (8)	5,630 $\pm$ 20b (5.7)	335 $\pm$ 4b (1.6)	137 $\pm$ 3a (1.4)	74 $\pm$ 3b (2)	19 $\pm$ 2a (2.9)	7,050 $\pm$ 77b (3.2)

Data are obtained from PIXE spectra from these regions using a full nonlinear deconvolution procedure. Selected regions: R0, whole region of the map shown in Figure 3, covering male reproductive organs (without testes); R1, vas deferens, vas efferens, and ejaculatory duct; R2, seminal vesicles; R3, accessory gland. Detection limits (99%) are given in parentheses. Different letters denote significant differences between selected regions at $P < 0.05$.

Table 4. Average mineral element concentrations (mean $\pm$ SD in mg kg^{-1}) in selected parts of the leaf of *Berkheya coddii* (*B.c.*) and various internal organs of *Epilachna nylanderi* (*E.n.*) and *Chrysolina clathrata* (*C.c.*)

	Species	S	Cl	K	Ca	Mn	Fe	Ni	Cu	Zn
B.c.	Total leaf	ND	35,950	5,730	7,850	99	609	23,110	82	32
B.c.	Mesophyll[a]	4,550 $\pm$ 160	40,000 $\pm$ 520	52,300 $\pm$ 330	7,600 $\pm$ 180	20 $\pm$ 10	113 $\pm$ 3.5	17,3 $\pm$ 46	ND	50 $\pm$ 30
E.n.	Midgut	2,900 $\pm$ 661*	3,700 $\pm$ 157*	1,120 $\pm$ 157*	3,000 $\pm$ 66*	100 $\pm$ 1.2*	11 $\pm$ 3.6*	324 $\pm$ 9*	10 $\pm$ 2.2*	2,100 $\pm$ 104*
C.c.		6,580 $\pm$ 504	5,180 $\pm$ 123	14,060 $\pm$ 331	235 $\pm$ 18	4 $\pm$ 2	129 $\pm$ 6	16 $\pm$ 2	36 $\pm$ 3	64 $\pm$ 5
E.n.	Malpighian tubules	1,460 $\pm$ 567*	14,750 $\pm$ 110*	8,770 $\pm$ 65*	7,790 $\pm$ 56*	386 $\pm$ 8*	114 $\pm$ 4.2*	126 $\pm$ 4.2*	11 $\pm$ 2*	2,130 $\pm$ 31*
C.c.		8,760 $\pm$ 2,260	6,140 $\pm$ 776	36,060 $\pm$ 106	554 $\pm$ 74	23 $\pm$ 19	330 $\pm$ 19	40 $\pm$ 23.3	33 $\pm$ 29	866 $\pm$ 35
E.n.	Brain ganglia	4,670 $\pm$ 123*	1,800 $\pm$ 246*	12,520 $\pm$ 113*	271 $\pm$ 47	2.6 $\pm$ 3.9*	105 $\pm$ 6	152 $\pm$ 15*	376 $\pm$ 10.5	583 $\pm$ 7.5
C.c.		9,270 $\pm$ 369	6,790 $\pm$ 164	16,100 $\pm$ 324	386 $\pm$ 10	1.5 $\pm$ 0.5	121 $\pm$ 3	6.9 $\pm$ 0.5	7.3 $\pm$ 0.5	39 $\pm$ 2
E.n.	Testes	8,200 $\pm$ 1,410	4,080 $\pm$ 260	13,650 $\pm$ 103*	341 $\pm$ 28*	3 $\pm$ 0.6	57 $\pm$ 1.5	4 $\pm$ 0.7	296 $\pm$ 4	122 $\pm$ 2.5*
C.c.		6,250 $\pm$ 140	6,310 $\pm$ 111	16,430 $\pm$ 433	107 $\pm$ 16	2.7 $\pm$ 0.5	77 $\pm$ 2	5 $\pm$ 1	230 $\pm$ 5	77 $\pm$ 1
E.n.	Other male	2,540 $\pm$ 749	4,550 $\pm$ 210*	14,770 $\pm$ 131*	1,320 $\pm$ 6*	8.6 $\pm$ 1.3*	110 $\pm$ 2.7	66 $\pm$ 2*	9.7 $\pm$ 1.3*	82 $\pm$ 2.7
E.n.[b]	reproductive organs	3,420 $\pm$ 515	844 $\pm$ 46*	4,530 $\pm$ 32*	4,810 $\pm$ 24*	302 $\pm$ 6.7*	135 $\pm$ 2.2	56 $\pm$ 2.1*	17 $\pm$ 1.3	6,020 $\pm$ 57*
C.c.		6,820 $\pm$ 266	3,520 $\pm$ 78	13,100 $\pm$ 255	245 $\pm$ 13	1.6 $\pm$ 0.9	81 $\pm$ 2	12 $\pm$ 1	29 $\pm$ 2*	136 $\pm$ 4

ND, not determined.
*Significant differences between the species ($P < 0.05$).
[a]Data from Mesjasz-Przybyłowicz et al. (2001) and Mesjasz-Przybyłowicz et al. (2004).
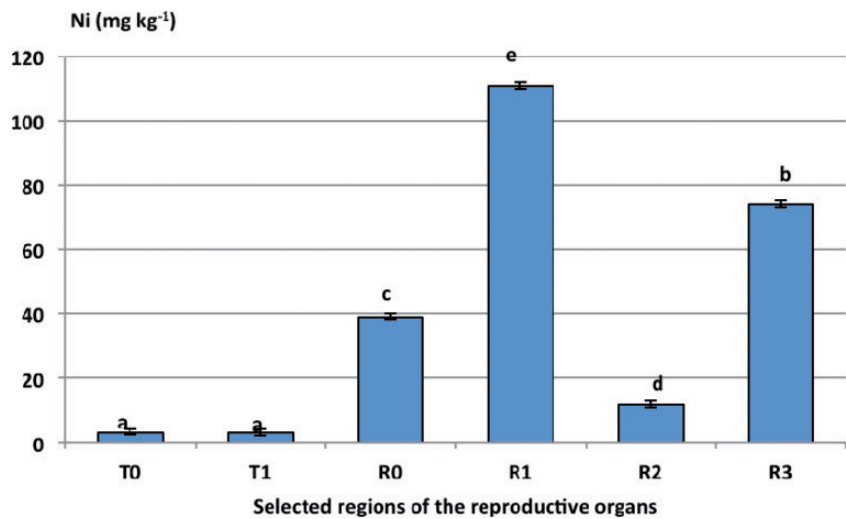[b]Insects fed on leaves enriched with Zn.

Fig. 4. Mean concentration of Ni (mg kg^{-1}) in selected regions of *Epilachna nylanderi* male reproductive tract. Explanation of the abbreviated names of the regions are given in Figures 2 and 3. Different letters denote significant differences between the organs at $P < 0.05$.

E. nylanderi was nearly the same as in *C. clathrata*, but this latter species also had lower Ni levels in the accessory reproductive structures, suggesting better protection against Ni than that of *E. nylanderi* (Table 4).

Ni concentrations in the brain ganglia of *E. nylanderi* were lower than in the midgut and at similar levels as in the Malpighian tubules (Tables 3 and 4). Comparison with the data obtained for *C. clathrata* (Migula et al. 2011) suggests worse protection of the brain against Ni toxicity (Table 4). Total elimination of the remains of quickly coagulating hemolymph from external structures of the examined CNS was not possible without washing the isolated organs. The higher concentration of Ni found in the region of interganglionic neural connectives probably also came from a coagulated hemolymph (N3 and N4; Figs. 1 and 5).
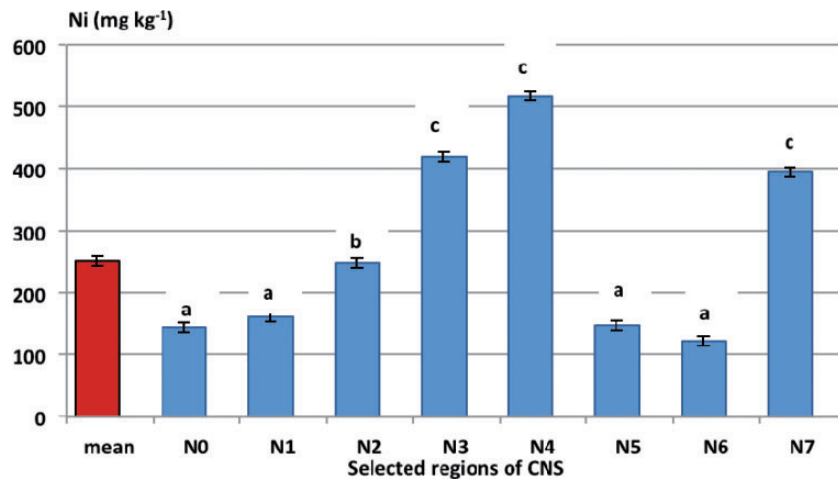
Fig. 5. Mean concentration of Ni (mg kg^{-1}) in selected regions of *E. nylanderi* CNS. Explanation of the abbreviated names of the regions is given in Figure 1. Different letters denote significant differences ($P < 0.05$) between selected parts of the CNS.

These structures, as well as the ganglia of the CNS, are well protected from direct inflow of external metals through an effective brain–blood barrier. The border between blood and neurons is about 10 times thicker than those separating nerve cells of mammals (Nation 2001). This is why the concentrations of ions on the external side of neuronal membrane and inside the neurons could differ from those in the hemolymph. The open insect circulatory system forces a strong isolation of the neuronal microenvironment using a network of fluid-filled clefts connected to the glial cells. Any disturbance of mineral transport could also influence the neurosecretory function of the main ganglia and may affect a variety of the physiological functions of the insect. This is also the reason why high concentrations of K determined in this study reflect external, not internal, levels in the analyzed samples.

Low bioconcentration ratio (bioconcentration factor) of Ni in the analyzed organs of *E. nylanderi* suggests that insects can efficiently deal with excessive amounts of metal. The low Ni concentration (86 mg kg^{-1}) was also reported in the brain of grasshopper (*Stenoscepa* sp.) larvae. Micro-PIXE analysis indicated less Ni in the optic lobe of the brain (31 mg kg^{-1}) than in the cerebral ganglia (246 mg kg^{-1}; Augustyniak et al. 2008). These results agree with the pattern of Ni distribution found in the CNS of *E. nylanderi* (Fig. 2). It is worth adding that only traces of Ni (1.4 mg kg^{-1}) were found in the heads of the thrips, *Haplothrips acanthoscelis*, the species that feeds on the leaves of *B. coddii* by puncturing them and sucking up liquid concentrations (Przybyłowicz et al. 2004).

Micro-PIXE analyses made possible comparisons of the quantitative variability and interactions of metals in different organs of *E. nylanderi*. The Ca/Ni ratio was very high in testis (87.4) and other internal male reproductive organs (73.1), whereas in the CNS, it was nearly balanced (1.1). This seems logical because more Ca in the reproductive system is needed to support intensive metabolic processes generated by cell division and the synthesis of various compounds supporting vitality of the germ cells and their transport within the reproductive tracts (Nation 2001). A similar effect was observed for Cu for which the concentration in the testis is more than 70 times higher than that of Ni. The highest Fe/Ni ratio in the testis (14.6) could also be related to the transport mechanisms of metals and Fe metabolism (Nichol et al. 2002). Insects kept on a diet without surplus of Zn had a low Zn/Ni ratio, suggesting that Zn was replaced by Ni, with possible adverse effects on enzymes that require Zn as a cofactor (Migula et al. 2004, Augustyniak et al. 2006).

The time of total development of *E. nylanderi* in similar laboratory conditions is nearly twice as long as observed for *C. clathrata*, 50.6 versus 25.0 d (Nakonieczny 2007). In comparison with *C. clathrata*, micro-PIXE analysis indicated weaker tolerance of the first species to the excess of Ni in the diet, reflected by higher concentrations of this metal in reproductive and neural organs. These differences may derive from various phylogenetic developments of the compared insects. *C. clathrata* represents chrysomelid beetles, which developed earlier as herbivores, whereas among generally carnivorous coccinellids, *E. nylanderii* represents a monophyletic group of herbivorous Epilachninae.

References Cited

Augustyniak, M., J. Juchimiuk, W. J. Przybyłowicz, J. Mesjasz-Przybyłowicz, A. Babczyńska, and P. Migula. 2006. Zinc-induced DNA damage and the distribution of metals in the brain of grasshoppers by the comet assay and micro-PIXE. Comp. Biochem. Physiol. 144: 242–251.

Augustyniak, M., J. Mesjasz-Przybyłowicz, M. Nakonieczny, M. Dybowska, W. J. Przybyłowicz, and P. Migula. 2002. Food relations between *Chrysolina pardalina* and *Berkheya coddii*—a nickel hyperaccumulator from South-African ultramafic outcrops. Fresen. Environ. Bull. 11: 85–90.

Augustyniak, M., W. Przybyłowicz, J. Mesjasz-Przybyłowicz, M. Tarnawska, P. Migula, E. Głowacka, and A. Babczyńska. 2008. Nuclear microprobe studies of grasshopper feeding on nickel hyperaccumulating plants. X-Ray Spectrom. 219–220: 57–66.

Bagatto, G., and J. D. Shorthouse. 1996. Accumulation of Cu and Ni in successive stages of *Lymantria dispar* L. (Lymantriidae, Lepidoptera) near ore smelters at Sudbury, Ontario, Canada. Environ. Pollut. 92: 7–12.

Beanland, L., P. L. Phelan, and S. Salminen. 2003. Micronutrient interactions on soybean growth and the developmental performance of three insect herbivores. Environ. Entomol. 32: 641–651.

Boyd, R. S. 2004. Ecology of metal hyperaccumulation. New Phytol. 162: 563–567.

Boyd, R. S. 2007. The defense hypothesis of elemental hyperaccumulation: status, challenges and new directions. Plant Soil 293: 153–176.

Boyd, R. S. 2009. High-nickel insects and nickel hyperaccumulator plants: a review. Insect Sci. 16: 19–31.

Boyd, R. S., and S. N. Martens. 1998. The significance of metal hyperaccumulation for biotic interactions. Chemoecology 9: 1–7.

Chung, J., D. J. Haile, and M. Wessling-Resnick. 2004. Copper-induced ferroportin-1491 expression in J774 macrophages is associated with increased iron efflux. Proc. Natl. Acad. Sci. USA. 101: 2700–2705.

Currie, L. A. 1968. Limits for qualitative detection and quantitative determination: application to radiochemistry. Anal. Chem. 40: 586–593.

Das, K. K., S. N. Das, and S. A. Dhundasi. 2008. Nickel, its adverse health effects & oxidative stress. Indian J. Med. Res. 128: 412–425.

Davey, K. G. 1985. The male reproductive tract, pp. 1–14. *In* G. A. Kerkut and L. I. Gilbert (eds.), Comprehensive insect physiology biochemistry and pharmacology, vol. 1, Pergamon Press, New York.

Doolittle, L. R. 1986. A semiautomatic algorithm for Rutherford, Oxford backscattering spectrometry. Nucl. Instrum. Methods Phys. Res. B 15: 227–231.

Giorgi, J. A., N. J. Vandenberg, J. V. McHugh, J. A. Forrester, S. A. Ślipiński, K. B. Miller, L. R. Shapiro, and M. F. Whiting. 2009. The evolution of food preference in Coccinellidae. Biol. Control 51: 215–231.

Green, I. D., A. Diaz, and M. Tibbett. 2010. Factors affecting the concentration in seven spotted ladybirds (*Coccinella septempunctata* L.) of Cd and Zn transferred through the food chain. Environ. Pollut. 158: 135–141.

Jhee, E. M., R. S. Boyd, M. D. Eubanks, and M. A. Davis. 2006. Nickel hyperaccumulation by *Streptanthus polygaloides* protects against the folivore *Plutella xylostella* (Lepidoptera: Plutellidae). Plant Ecol. 183: 91–104.

Klag, J., J. Mesjasz-Przybyłowicz, M. Nakonieczny, and M. Augustyniak. 2002. Ultrastructure of the midgut of the chrysomelid beetle *Chrysolina pardalina,* pp. 685–686. *In* R. Cross (ed.), Proceedings of the 15th International Congress on Electron Microscopy, Microscopy Society of Southern Africa, Durban, South Africa.

Kozlov, M. V., E. Haukijoja, and E. F. Kovnatsky. 2000. Uptake and excretion of nickel and copper by leaf-mining larvae of *Eriocrania semipurpurella* (Lepidoptera: Eriocranidae) feeding on contaminated birch foliage. Environ. Pollut. 108: 303–310.

Kramarz, P. 1999. The dynamics of accumulation and decontamination of cadmium and zinc in carnivorous invertebrates: 1. The ground beetle, *Poecilus cupreus* L. Bull. Environ. Contam. Toxicol. 4: 531–538.

Levy, R., and H. L. Cromroy. 1973. Concentrations of some major and trace elements in forty one species of adult and immature insects by atomy absorption spectroscopy. Ann. Entomol. Soc. Am. 66: 523–526.

Makgale, M. 2008. Nuclear microprobe techniques in studies of toxic effects in insect *Epilachna* sp. M.Sc. thesis, Centre for Applied Radiation Science and Technology (CARST), University of North-West, Mafikeng, South Africa.

Mattson, W. J., and J. M. Scriber. 1986. Nutritional ecology of insect folivores of woody plants, pp. 105–146. *In* F. Slansky, Jr. and J. G. Rodriguez (eds.), Nutritional ecology of insects spiders, mites, spiders and related invertebrates, John Wiley & Sons, New York, Toronto.

Mesjasz-Przybyłowicz, J., and W. J. Przybyłowicz. 2001. Phytophagous insects associated with the Ni-hyperaccumulating plant *Berkheya coddii* (Asteraceae) in Mpumalanga, South Africa. S. Afr. J. Sci. 97: 596–598.

Mesjasz-Przybyłowicz, J., W. J. Przybyłowicz, and C. A. Pineda. 2001. Nuclear microprobe studies of elemental distribution in apical leaves of the Ni hyperaccumulator *Berkheya coddii*. S. Afr. J. Sci. 97: 591–593.

Mesjasz-Przybyłowicz, J., and W. J. Przybyłowicz. 2011. PIXE and metal hyperaccumulation: from soil to plants and insects. X-Ray Spectrum. 40: 181–185.

Mesjasz-Przybyłowicz, J., W. Przybyłowicz, M. Augustyniak, B. Ostachowicz, M. Nakonieczny, and P. Migula. 2002. Trace elements in the chrysomelid beetle (*Chrysolina pardalina*) and its Ni-hyperaccumulating host-plant (*Berkheya coddii*). Fresen. Environ. Bull. 11: 78–84.

Mesjasz-Przybyłowicz, J., M. Nakonieczny, P. Migula, M. Augustyniak, M. Tarnawska, U. W. Reimold, C. Koeberl, W. Przybyłowicz, and E. Głowacka. 2004. Uptake of cadmium, lead nickel and zinc from soil and water solutions by the nickel hyperaccumulator *Berkheya coddii*. Acta Biol. Cracoviensia Ser. Bot. 46: 75–85.

Migula, P. 1996. Trace metals in animals: an overview on essentiality transport, accumulation and adaptive mechanisms. Biol. Bull. 33: 9–13.

Migula, P., M. Nakonieczny, M. Augustyniak, M. Tarnawska, W. J. Przybyłowicz, and J. Mesjasz-Przybyłowicz. 2011. Micro-PIXE studies of Ni-elimination strategies in representatives of two families of beetles feeding on Ni-hyperaccumulating plant *Berkheya coddii*. X-Ray Spectrum. 40: 194–197.

Migula, P., P. Łaszczyca, M. Augustyniak, G. Wilczek, K. Rozpędek, A. Kafel, and M. Wołoszyn. 2004. Antioxidative defence enzymes in beetles from a metal pollution gradient. Biol. Brat. 59: 645–654.

Migula, P., W. J. Przybyłowicz, J. Mesjasz-Przybyłowicz, M. Augustyniak, M. Nakonieczny, E. Głowacka, and M. Tarnawska. 2007. Micro-PIXE studies of elemental distribution in sap-feeding insects associated with Ni hyperaccumulator, *Berkheya coddii*. Plant Soil 293: 197–207.

Morrey, D. R., K. Balkwill, and M. J. Balkwill. 1989. Studies on serpentine flora. S. Afr. J. Bot. 55: 171–177.

Nakonieczny, M. 2007. Structural and functional adaptations of *Chrysolina pardalina* (Chrysomelidae; Coleoptera) to development on nickel hyperaccumulator *Berkheya coddii* (Asteraceae)—a comparative study with *Chrysolina herbacea*. Wydawnictwo Uniwersytetu Śląskiego, Katowice, Poland.

Nation, J. L. 2001. Insect physiology and biochemistry. CRC Press, Boca Raton, New York.

Nichol, H., J. H. Law, and J. J. Winzerling. 2002. Iron metabolism in insects. Annu. Rev. Entomol. 47: 535–559.

Nieboer, E., and D. H. S. Richardson. 1980. The replacement of the non-descriptive term "Heavy Metals" by a biologically and chemically significant classifications of metals ions. Environ. Pollut. 1: 3–26.

Nunez, M. T., V. Tapia, A. Rojas, P. Aguirre, F. Gomez, and F. Nualart. 2010. Iron supply determines apical/basolateral membrane distribution of intestinal iron transporters DMT1 and ferroportin 1. Am. J. Physiol. Cell Physiol. 298: C477–C485.

Peterson, L. R., V. A. Trivet, J. M. Baker, and A. J. Pollard. 2003. Spread of metals through an invertebrate food chain as influenced by a plant that hyperaccumulates nickel. Chemoecology 13: 103–108.

Prozesky, V. M., W. J. Przybyłowicz, E. Van Achterbergh, C. L. Churms, C. A. Pineda, K. A. Springhorn, J. V. Pilcher, C. G. Ryan, J. Kritzinger, H. Schmitt, et al. 1995. The NAC nuclear microprobe facility. Nucl. Instrum. Methods Phys. Res. B 104: 36–42.

Przybyłowicz, W. J., J. Mesjasz-Przybyłowicz, C. A. Pineda, C. L. Churms, K. A. Springhorn, and V. M. Prozesky. 1999. Biological applications of the NAC nuclear microprobe. X-Ray Spectrum. 28: 237–243.

Przybyłowicz, W.J., J. Mesjasz-Przybyłowicz, P. Migula, E. Głowacka, M. Nakonieczny, and M. Augustyniak. 2003. Functional analysis of metals distribution in organs of the beetle *Chrysolina pardalina* exposed to excess of nickel by Micro-PIXE. Nucl. Instrum. Methods Phys. Res. B 210: 343–348.

Przybyłowicz, W. J., J. Mesjasz-Przybyłowicz, P. Migula, K. Turnau, M. Nakonieczny, M. Augustyniak, and E. Głowacka. 2004. Elemental microanalysis in ecophysiology using ion beam. Nucl. Instrum. Methods Phys. Res. B 219–220: 57–66.

Przybyłowicz, W. J., J. Mesjasz-Przybyłowicz, P. Migula, M. Nakonieczny, M. Augustyniak, M. Tarnawska, K. Turnau, P. Ryszka, E. Orłowska, S. Zubek, et al. 2005. Micro-PIXE in ecophysiology. X-Ray Spectrum. 34: 285–289.

Rost-Roszkowska, M., I. Poprawa, J. Klag, P. Migula, J. Mesjasz-Przybyłowicz, and W. Przybyłowicz. 2008. Degeneration of the midgut epithelium in *Epilachna cf. nylanderi* (Insecta, Coccinellidae): apoptosis, autophagy and necrosis. Can. J. Zool. 86: 1179–1188.

Rost-Roszkowska, M., I. Poprawa, J. Klag, P. Migula, J. Mesjasz-Przybyłowicz, and W. Przybyłowicz. 2010. Differentiation of regenerative cells in the midgut epithelium of *Epilachna cf. nylanderi* (Mulsant 1850) (Insecta, Coleoptera, Coccinellidae). Folia Biol. 58: 209–216.

Ryan, C. G. 2000. Quantitative trace element imaging using PIXE and the nuclear microprobe. Int. J. Imaging Syst. Technol. 11: 219–230.

Ryan, C. G., and D. N. Jamieson. 1993. Dynamic analysis: on-line quantitative PIXE microanalysis and its use in overlap-resolved elemental mapping. Nucl. Instrum. Methods Phys. Res. B 77: 203–214.

Ryan, C. G., D. N. Jamieson, C. L. Churms, and J. V. Pilcher. 1995. A new method for on-line true-elemental imaging using PIXE and the proton microprobe. Nucl. Instrum. Methods Phys. Res. B 104: 157–165.

Ryan, C. G., D. R. Cousens, S. H. Sie, W. L. Griffin, G. F. Suter, and E. Clayton. 1990. Quantitative PIXE microanalysis of geological material using the CSIRO proton microprobe. Nucl. Instrum. Methods Phys. Res. B 47: 55–71.

Tabashnik, B. E., and F. Slansky, Jr. 1986. Nutritional ecology of forb foliage-cheving insects, pp. 75–103. *In* F. Slansky, Jr. and J. G. Rodriguez (eds.), Nutritional ecology of insects spiders, mites, spiders and related invertebrates, John Wiley & Sons, New York, Toronto.

Troadec, M. B., D. M. Ward, E. Lo, J. Kaplan, and I. De Domenico. 2010. Induction of FPN1 transcription by MTF-1 reveals a role for ferroportin in transition metal efflux. Blood 116: 4657–4664.

Valko, M., H. Morris, and M. T. D. Cronin 2005. Metals, toxicity and oxidative stress. Curr. Med. Chem. 12: 1161–1208.

Van Achterbergh, E., C. G. Ryan, J. J. Gurney, and A. P. Le Roex. 1995. PIXE profiling, imaging and analysis using the NAC proton microprobe: unraveling mantle eclogites. Nucl. Instrum. Methods Phys. Res. B 104: 415–426.

Vijver, M., C. A. M. Van Gestel, R. P. Lanno, N. Van Straalen, and W. J. Peijneburg. 2004. Internal metal sequestration and its ecotoxicological relevance. Environ. Sci. Technol. 38: 4705–4712.

Zawisza-Raszka, A., and B. Doleżych. 2008. Acetylcholinesterase, catalase and glutathione S-transferase activity in beet armyworm *Spodoptera exigua* exposed to nickel and/or diazinon. Acta Biol. Hung. 59: 31–45.